hv *photonics*

MDPI

Letter

A Robust Method for Adjustment of Laser Speckle Contrast Imaging during Transcranial Mouse Brain Visualization

Vyacheslav Kalchenko [1,*,†] , Anton Sdobnov [2,†] , Igor Meglinski [2,3,4,5,6] , Yuri Kuznetsov [1], Guillaume Molodij [1] and Alon Harmelin [1]

[1]   Department of Veterinary Resources, Weizmann Institute of Science, 76100 Rehovot, Israel
[2]   Optoelectronics and Measurement Techniques Laboratory, University of Oulu, 90570 Oulu, Finland
[3]   Interdisciplinary Laboratory of Biophotonics, National Research Tomsk State University,
       634050 Tomsk, Russia
[4]   Institute of Engineering Physics for Biomedicine (PhysBio), National Research Nuclear University (MEPhI),
       115409 Moscow, Russia
[5]   Aston Institute of Materials Research, School of Engineering and Applied Science, Aston University,
       Birmingham B4 7ET, UK
[6]   School of Life and Health Sciences, Aston University, Birmingham B4 7ET, UK
*   Correspondence: a.kalchenko@weizmann.ac.il; Tel.: +972-8-934-3228
†   These two authors contributed equally to this work.

check for updates

Abstract: Laser speckle imaging (LSI) is a well-known and useful approach for the non-invasive visualization of flows and microcirculation localized in turbid scattering media, including biological tissues (such as brain vasculature, skin capillaries etc.). Despite an extensive use of LSI for brain imaging, the LSI technique has several critical limitations. One of them is associated with inability to resolve a functionality of vessels. This limitation also leads to the systematic error in the quantitative interpretation of values of speckle contrast obtained for different vessel types, such as sagittal sinus, arteries, and veins. Here, utilizing a combined use of LSI and fluorescent intravital microscopy (FIM), we present a simple and robust method to overcome the limitations mentioned above for the LSI approach. The proposed technique provides more relevant, abundant, and valuable information regarding perfusion rate ration between different types of vessels that makes this method highly useful for in vivo brain surgical operations.

Keywords: cerebral blood vessels; middle cerebral artery; transcranial imaging; in vivo fluorescence imaging; non-invasive optical imaging; speckle contrast

1. Introduction

During the last decade, a highly detailed in vivo imaging of the brain vascular network (arteries through capillaries to veins) became a hot topic for the biophotonics community. Nowadays, a large amount of non-invasive optical-based imaging techniques, such as optical coherence tomography [1], photoacoustic microscopy [2], photo-acoustic tomography [3], multiphoton microscopy [4], laser speckle imaging (LSI) [5], and others, are emerging for the use in clinical and preclinical brain-related studies. In fact, in current practice, the invasive techniques, like a surgical removal of skin or/and the skull, are usually performed to improve the image contrast of organization of cortical map and/or brain vascular network [6–8]. Thus, imaging of cerebral blood vessels through the intact skull still remains a complex and challenging task, usually requiring expensive equipment.

Recently, the cost-effective multi-modal experimental setup, combining a laser speckle imaging (LSI) approach and fluorescent intravital microscopy (FIM) with a unique possibility to observe small, down to 1 to 5 μm/s, and post-mortal blood flows, has been introduced [9]. LSI allows non-invasive mapping of blood flow and perfusion visualization in various biomedical tissues in real time [10], whereas the fluorescence-based angiography, like FIM, tracks the temporal distribution of a fluorescent dye through the vasculature and thereby provides functional information about hemodynamics [11]. A combined use of LSI and FIM methods has been successfully applied for visualization of cerebral blood flow though the intact mice skull [9]. This approach has been also used for observation of blood and lymph micro-flows in tumors [12–14], and for visualization of skin vascular network [15] and tumor surroundings [16]. Moreover, it was demonstrated that this approach allows visualization and quantitative assessment of vascular reaction in an immediate response to the optical clearing agents, chemical agents, and potential allergens interaction with the skin [17]. The LSI–FIM system has been extensively used in the routine mouse ear swelling test (MEST) screenings [18].

Despite an extensive use of LSI–FIM in various biomedical applications, the LSI-based approach has several critical limitations. Typically, in the LSI experiment, due to the finite camera exposure time, the local dynamics of observed scatters leads to the blurring of speckle patterns. This blurring, consequently, decreases the speckle contrast (K), but allows quantifying of the flow rate, and is defined as [19]:

$$K = \frac{\sigma}{\langle I \rangle},\tag{1}$$

where σ is the intensity standard deviation and $\langle I \rangle$ is the mean intensity value. However, a presence of static tissue inclusions in observed object provides a systematic distortion in the quantitative interpretation of laser light fluctuations associated with the dynamic light scattering (i.e., scattering of light on the moving particles). This problem has been considered in [20–22]. Also, some noise factors such as physiological noise, hardware noise, environmental noise, etc., can impact the evaluation of laser speckle contrast [23].

Another serious limitation of LSI is the inability of the approach to determine the functionality of the vessels' types, such as sagittal sinus, arteries, and veins. This also often leads to an incorrect assessment and interpretation of brain images obtained by LSI. In particular, a number of brain LSI studies (see for example [6–8]) demonstrated that veins and arteries have a similar flow rate, whereas flow in the sagittal sinus was shown to be much more intensive than in both veins and arteries. In fact, the flow rate in veins and arteries is notably different and the sagittal sinus has the slowest flow rate comparing to the above-mentioned vascular beds [24]. Despite the fact that LSI technique is widely used for intraoperative monitoring of cerebral blood flow during neurosurgery [25–27], the described problem is discussed in only a few papers. The relative temporal minimum reflectance analysis of laser speckle images has been presented for functional identification of blood vessels in [28]. This approach requires the use of light source in the narrow spectral range 600–640 nm. Further, utilizing the cardiac pulse activity, the method of arteries and veins identification has been introduced in [29]. The alternative technique of different vessels types identification of the brain vasculature is based on the combine use of the LSI–FIM system [9]. In fact, all of the studies mentioned above do not overcome the problem of incorrect speckle contrast values interpretation.

In the current letter, we present a further development of the LSI–FIM technique for the transcranial mouse brain visualization by using the correction of speckle contrast values of the brain vasculature functional identification.

2. Materials and Methods

Figure 1a schematically presents the dual mode LSI–FIM imaging system, developed in-house. Here, the LSI mode utilized a 3 mW laser diode module (LDM808/3LJ, Roithner Lasertechnik, Vienna, Austria), emitting light at 808 nm, which was further expanded by a ground glass diffuser (Thorlabs, Newton, NJ, USA) and illuminated the mouse head. The charge-coupled device (CCD) camera (Pixelfly

QE, PCO, Kelheim, Germany, 1392 × 1024, pixel size: 6.4 μm) mounted by C-mount adaptor on top of the standard fluorescent zoom stereomicroscope SZX12 RFL2 (Olympus, Tokyo, Japan) with DF PLAPO 1× PF lenses (Olympus, Tokyo, Japa) was used for acquisition of gray-scale raw speckle images (400 frames per experiment) with 10 ms exposure time. It is important to notice that speckle contrast values obtained during the brain imaging are affected by the camera exposure time [30] as well as by the coherence properties of laser source. Due to the results presented in the reference [23], the exposure time in the range of 5–10 ms allows the high contrast to noise ratio to be achieved (CNR). Also, for maximization of the signal to noise ratio (SNR), the minimal speckle size must exceed the Nyquist criterion [31]. Thus, the minimal speckle size was 12.8 μm. So, for the described LSI mode, the minimal speckle contrast volume (dynamic region) and maximal speckle contrast volume (static region) were 0.02 and 0.48, respectively. The camera control and image acquisition were performed by utilizing CamWare (PCO, Kelheim, Germany). In the FIM mode, the mercury short arc lamp has been used as a light source. The excitation light was adjusted by optical filter at 460 to 490 nm and directed to the same area of the mouse head as in LSI mode via a diachronic mirror (DM-505, Croma, VT, USA). Further, the fluorescence light that passed through the emission band-pass filter at 510 to 550 nm was detected by the same CCD camera (see Figure 1). After fluorescein administration, 400 acquired raw images (exposure time: 50 ms per frame) were used for further analysis. The obtained LSI and FIM images were processed by a custom-developed algorithm in the offline regime using Fiji/ImageJ (image processing package [32]) software.

The algorithms for LSI and FIM modes image processing are well described in previous studies [9]. Briefly, in the LSI mode, the standard method of temporal statistical analysis of the laser speckle contrast has been employed (see Figure 1b). The mean value and standard deviation have been calculated for each pixel of 400 raw speckle frames stack (with 10 frames step) to obtain the final speckle contrast image. For the calculation of color-coded dynamic fluorescent (DF) images with the discrimination of functionality of different vessels types, the procedure schematically presented in Figure 1c has been performed. Firstly, a stack of 200 raw DF images (the first 10 s after fluorescein administration) was captured. Further, the obtained images were enhanced by noise reduction procedure, short-term fluctuations removing procedure, etc., utilizing Fiji custom-developed script. To discriminate functional types of brain vessels, the color coding, namely intensity-hue-saturation (IHS) model, has been applied. As soon as the time for the maximum intensity was calculated for each pixel of image stack, this time becomes encoded as a value of hue, representing the color in frame of the IHS coloring scheme. As far as the intensity maximum time for arteries and veins is different, discrimination between different types of brain vascular beds becomes possible utilizing such a color-coding scheme. Further, maximum intensity projection (MIP) has been calculated using a stack of raw fluorescent images to obtain anatomical pattern of blood vessels. After that, MIP was encoded as both intensity and saturation. Finally, IHS DF image was obtained using Fiji custom-developed script.

A CD1 nude female mouse aged between six to eight weeks from Envigo was used in the experiment. The animal was anesthetized with 10 mg/100 mg/kg ketamine (Vetoquinol, Lure, France) and xylazin (Eurovet Animal Health, Bladel, The Netherlands) by intra-peritoneal injection. After the injection of general anesthetics, an initial cut was made and the skin over the frontal, temporal, occipital, and parietal regions was removed by blunt dissection. Further, the exposed area of interest was constantly moistened with saline. Then, the mouse was placed under the microscope lens on a special mouse holder with a warming plate, which maintained a constant body temperature of 37 °C. For obtaining the DF images, a dose of 0.025 mg fluorescein in a volume of 100 μL was injected into the tail vein. In general, the duration of experimental measurements was less than 1.5 h, after which all animals were sacrificed by barbiturate overdose.
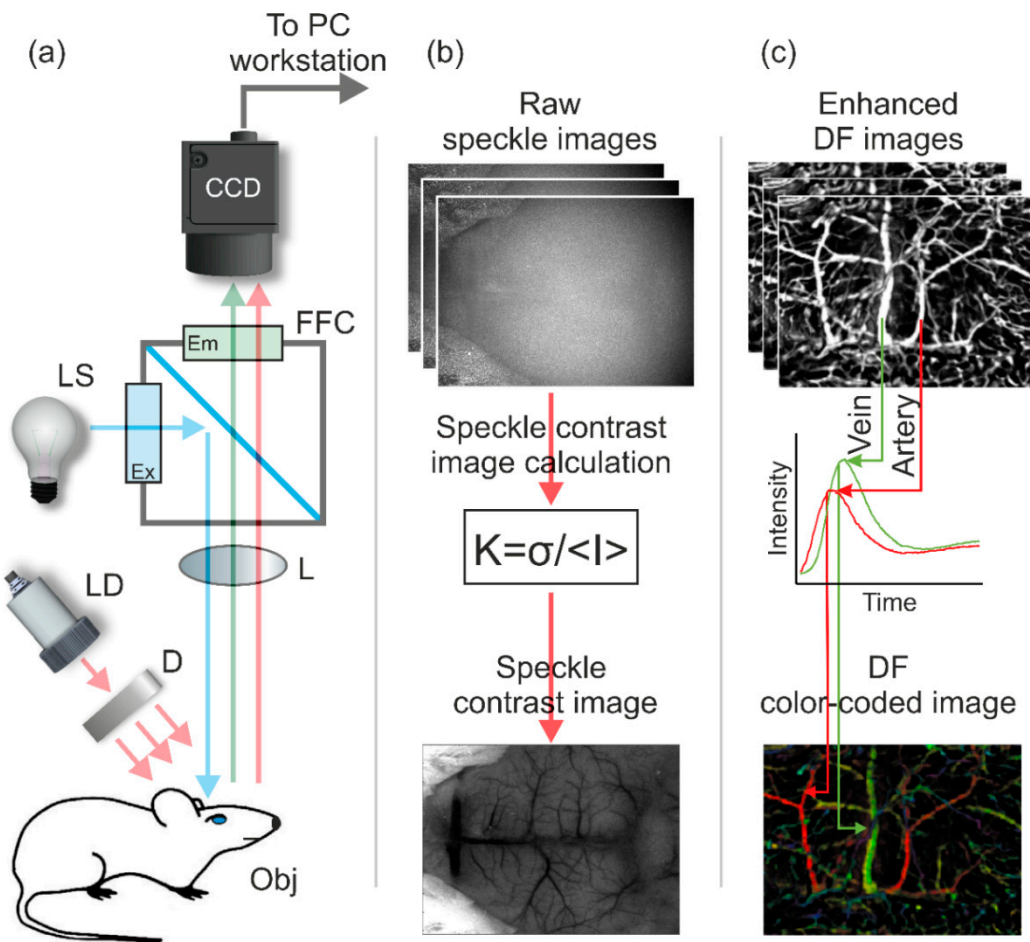
Figure 1. Schematic presentation of principles of operation of the combined laser speckle imaging and fluorescent intravital microscopy (LSI–FIM) experimental system used in the study (**a**): CCD–CCD camera, LS is the light source for fluorescence imaging, Ex is the excitation optical filter, Em is the emission band-pass filter, FFC is the fluorescence filter cube, L are the lens, D is the diffuser, LD is the laser diode for speckle imaging, Obj is the object of investigation. Principle of speckle contrast images calculation (**b**): CCD camera captured stack of raw speckle images. Further, speckle contrast images calculated using Equation (1) by a custom-developed algorithm in offline regime. (**c**) Principle of color-coded dynamic fluorescent (DF) images obtained with discrimination between different brain vessels types: CCD camera captured stack of fluorescent images during a 10 s after fluorescent material administration. Further, maximum intensity projection (MIP) has been identified for each pixel in the stack as a function of time. The graph shows florescence intensity as a function of time, illustrating the difference in arrival time between arteries (red) and veins (green). Further, DF color-coded image with discrimination between veins and arteries has been calculated using the intensity-hue-saturation (HIS) color model. Hue encodes time of maximal pixel intensity, whereas MIP is encoded as both intensity and saturation.

3. Results and Discussion

Figure 2a shows a color-coded DF image of the mouse brain for the first 10 s from the beginning of the experiment. Using the method described above, data from an image of the arterial and venous phases colored, respectively, as red and green. Color pallets were chosen for convenience of perception. Figure 2b shows the laser speckle contrast image of mouse brain vasculature for the same time period as on the DF image. The image has been colored in false color "hot" pallet for better clarity. Using both Figure 2a,b, it can be seen that perfusion in the veins is higher than in the arteries (see points 1–4 on Figure 2b). Moreover, sagittal sinus has the maximum perfusion rate compared to other types of

vessels (see point 5 on Figure 2b). As mentioned above, similar perfusion images of brain vasculature are commonly presented elsewhere, see for example [6–8]. In fact, the quantitative and/or functional interpretation of images is complicated and can lead to critical mistakes. In order to overcome this problem, we propose to use the images obtained in frame of the FIM mode for adjustment and further interpretation of LSI. FIM provides the temporal distribution and redistribution of a fluorescent material through the vasculature, which corresponds to the real perfusion rate in vessels. In this way, the speckle contrast value should proportionally depend on the time of the maximum fluorescence. Time corresponding to the maximum fluorescence value Tmax can be detected for each pixel of the image sequence. Further, it can be used for correction of the laser speckle contrast for various types of brain vasculature.

Figure 2c shows fluorescence time to maximum image for the first 10 s from the beginning of the experiment. Further, Tmax can be used as a reference to the real blood flow. For correction of the speckle contrast values in each pixel of the image, we propose to use the next equation:

$$Kcorr_{i,j} = \log(T\max_{i,j})K_{i,j},\qquad(2)$$

where $T\max_{i,j}$ is the fluorescence time to maximum for pixel (i, j), $K_{i,j}$ is the speckle contrast value for pixel (i, j), and $Kcorr_{i,j}$ is the speckle contrast value for pixel (i, j) after correction. The proposed equation was found experimentally. The variety of different functions were tested for correction of the speckle image. The multiplication by log (Tmax) was found to be the optimal one as it allowed the obtaining of the flow map, which has the flow distribution close how it is described in the literature [24].
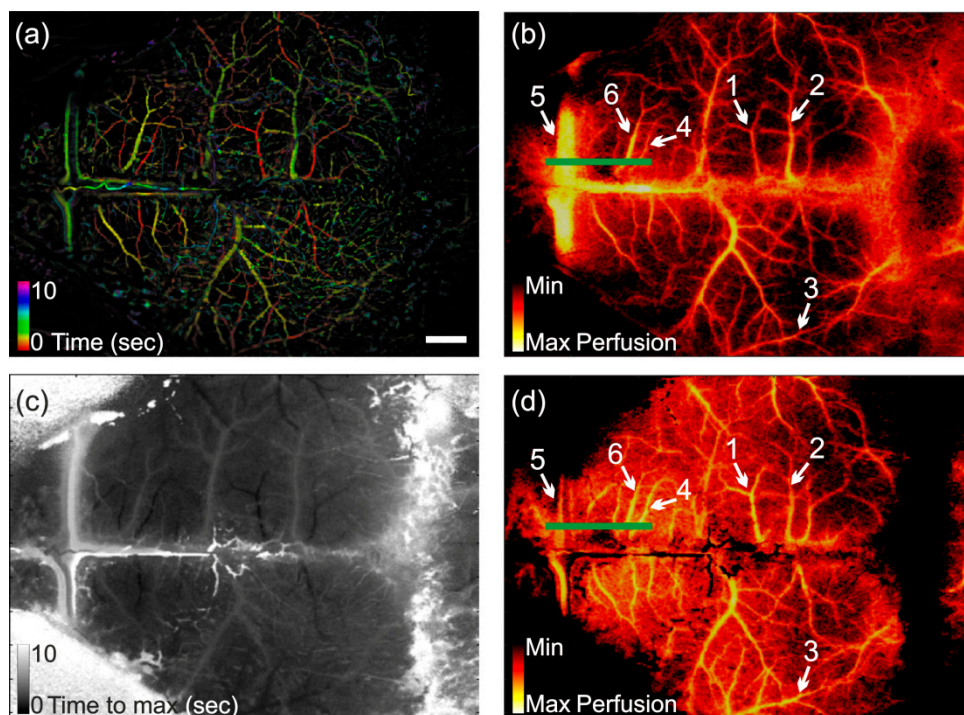

Figure 2. (**a**) Color-coded DF image of mouse brain distinguishing veins and arteries. Red colors correspond to arteries, whereas green colors correspond to the veins; (**b**) Speckle contrast image of mouse brain before correction procedure; (**c**) Fluorescence time to maximum image; (**d**) Speckle contrast image of mouse brain after correction procedure. Scale bar (white line) is equal to 1 mm. The green line represents the line for contrast intensity profiles calculation.

Figure 2d shows speckle contrast image of mouse brain vasculature after correction procedure utilizing Equation (2). As one can see, the perfusion in the veins is notably less than in the arteries (see Figure 2d, points 1–4). Moreover, perfusion rate in sagittal sinus significantly decreased (see Figure 2d,

see point 5). It should be also pointed out that perfusion values in the areas outside the vessels became higher. Figure 3 shows the line intensity profiles of the speckle contrast images before and after the correction procedure, calculated as described in [33]. The line intensity profiles were calculated along the green lines on the Figure 2b,d. From the intensity profile of the speckle contrast image calculated by traditional method, it is clearly seen that vein (point 6) and artery (point 4) intensities took close values (see Figure 3). The sagittal sinus took the greatest intensity value, as it was already mentioned above. As one can see, from the intensity profile of the speckle contrast image calculated using Equation (2), the artery intensity (point 4) increased compared to the vein intensity (point 6), while intensity of sagittal sinus was significantly decreased. Therefore, the proposed approach with the correction of speckle contrast values is more plausible and useful for transcranial assessment of functionality of brain vascular network in vivo.
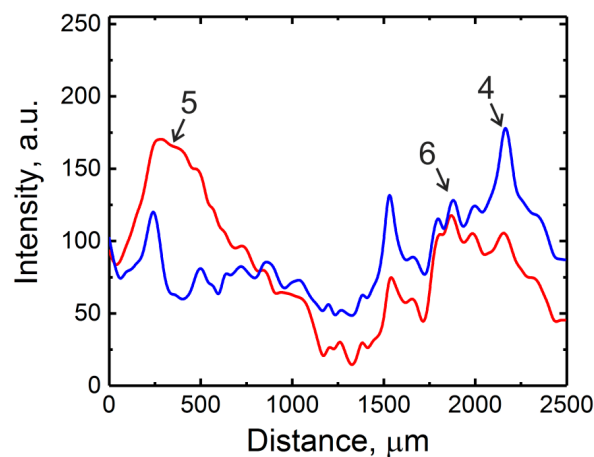

Figure 3. Contrast intensity profiles of lines (showed as the green lines in Figure 2b,d) across the speckle contrast images before and after the correction procedure. The red line corresponds to the contrast intensity profile of the speckle contrast image before the correction procedure. The blue line corresponds to the contrast intensity profile of the speckle contrast image after correction procedure. Points 4, 5, and 6 correspond to artery, sagittal sinus, and vein (showed as the same points in Figure 2b,d), respectively.

The proposed method still requires further development and improvement to become a real quantitative tool for noninvasive assessment of the brain vasculature. However, we believe that the proposed approach will allow for advanced visualization of the brain vasculature during neurosurgery. Also, the described technique can be highly useful for preclinical trials, especially in the development of the new central nervous system (CNS) drugs, and for analysis of cerebral circulation disorder models. Application of the machine learning approach [34] can further improve the correction results. Moreover, combined use of the proposed method with the optical clearing technique [35–38] will possibly allow for the fully noninvasive brain imaging of mice of up to six months of age.

4. Conclusions

To sum up, in the current letter, we have mainly focused on the introduction of a simple practical method for the functional interpretation of the blood perfusion in the brain vasculature. The combined use of the LSI–FIM system allowed adjusting of the transcranial laser speckle contrast imaging of mouse brain in vivo. The proposed method is not yet mature and still requires further development and improvement to become a real quantitative tool for noninvasive assessment of the brain vasculature. However, we believe that the described approach is highly useful for neurosurgery, as far as corrected speckle contrast images provide more relevant and adequate information on perfusion rate ration between different types of vessels.

References

1. Vakoc, B.J.; Lanning, R.M.; Tyrrell, J.A.; Padera, T.P.; Bartlett, L.A.; Stylianopoulos, T.; Munn, L.L.; Tearney, G.J.; Fukumura, D.; Jain, R.K.; et al. Three-dimensional microscopy of the tumor microenvironment in vivo using optical frequency domain imaging. *Nat. Med.* **2009**, *15*, 1219–1223. [CrossRef] [PubMed]
2. Stein, E.W.; Maslov, K.; Wang, L.V. Noninvasive, in vivo imaging of the mouse brain using photoacoustic microscopy. *J. Appl. Phys.* **2009**, *105*, 102027. [CrossRef] [PubMed]
3. Burton, N.C.; Patel, M.; Morscher, S.; Driessen, W.H.; Claussen, J.; Beziere, N.; Jetzfellner, T.; Taruttis, A.; Razansky, D.; Bednar, B.; et al. Multispectral opto-acoustic tomography (MSOT) of the brain and glioblastoma characterization. *NeuroImage* **2013**, *65*, 522–528. [CrossRef] [PubMed]
4. Harb, R.; Whiteus, C.; Freitas, C.; Grutzendler, J. In vivo imaging of cerebral microvascular plasticity from birth to death. *J. Cereb. Blood Flow. Metab.* **2013**, *33*, 146–156. [CrossRef] [PubMed]
5. Towle, E.L.; Richards, L.M.; Kazmi, S.S.; Fox, D.J.; Dunn, A.K. Comparison of indocyanine green angiography and laser speckle contrast imaging for the assessment of vasculature perfusion. *Neurosurgery* **2012**, *71*, 1023–1030. [CrossRef] [PubMed]
6. Abdurashitov, A.S.; Lychagov, V.V.; Sindeeva, O.A.; Semyachkina-Glushkovskaya, O.V.; Tuchin, V.V. Histogram analysis of laser speckle contrast image for cerebral blood flow monitoring. *Front. Optoelectr.* **2015**, *8*, 187–194. [CrossRef]
7. Semyachkina-Glushkovskaya, O.; Abdurashitov, A.; Pavlov, A.; Shirokov, A.; Navolokin, N.; Pavlova, O.; Gekalyuk, M.; Ulanova, N.; Shushunova, A.; Bodrova, A.; et al. Laser speckle imaging and wavelet analysis of cerebral blood flow associated with the opening of the blood–brain barrier by sound. *Chin. Opt. Lett.* **2017**, *15*, 090002. [CrossRef]
8. Gnyawali, S.C.; Blum, K.; Pal, D.; Ghatak, S.; Khanna, S.; Roy, S.; Sen, C.K. Retooling laser speckle contrast analysis algorithm to enhance non-invasive high resolution laser speckle functional imaging of cutaneous microcirculation. *Sci. Rep.* **2017**, *7*, 41048. [CrossRef] [PubMed]
9. Kalchenko, V.; Israeli, D.; Kuznetsov, Y.; Harmelin, A. Transcranial optical vascular imaging (TOVI) of cortical hemodynamics in mouse brain. *Sci. Rep.* **2014**, *4*, 5839. [CrossRef] [PubMed]
10. Boas, D.A.; Dunn, A.K. Laser speckle contrast imaging in biomedical optics. *J. Biomed. Opt.* **2010**, *15*, 011109. [CrossRef]
11. Glover, S.J.; Maude, R.J.; Taylor, T.E.; Molyneux, M.E.; Beare, N.A. Malarial retinopathy and fluorescein angiography findings in a Malawian child with cerebral malaria. *Lancet Infect. Dis.* **2010**, *10*, 440. [CrossRef]
12. Meglinski, I.; Kalchenko, V.V.; Kuznetsov, Y.L.; Kuznik, B.I.; Tuchin, V.V. Towards the nature of biological zero in the dynamic light scattering diagnostic techniques. *Doklady Phys.* **2013**, *58*, 323–326. [CrossRef]
13. Kalchenko, V.; Kuznetsov, Y.; Harmelin, A.; Meglinski, I.V. Label free in vivo laser speckle imaging of blood and lymph vessels. *J. Biomed. Opt.* **2012**, *17*, 050502. [CrossRef] [PubMed]
14. Kalchenko, V.; Kuznetsov, Y.L.; Meglinski, I. Visualization of blood and lymphatic vessels with increasing exposure time of the detector. *Quantum Electron.* **2013**, *43*, 679–682. [CrossRef]
15. Kalchenko, V.; Madar-Balakirski, N.; Meglinski, I.; Harmelin, A. In vivo characterization of tumor and tumor vascular network using a multi-mode imaging approach. *J. Biophotonics* **2011**, *4*, 645–649. [PubMed]

16. Kalchenko, V.; Ziv, K.; Addadi, Y.; Madar-Balakirski, N.; Meglinski, I.; Neeman, M.; Harmelin, A. Combined application of dynamic light scattering imaging and fluorescence intravital microscopy in vascular biology. *Laser Phys. Lett.* **2010**, *7*, 603–606. [CrossRef]

17. Kuznetsov, Y.L.; Kalchenko, V.V.; Astaf'eva, N.Y.G.E.; Meglinski, I.V. Optical diagnostics of vascular reactions triggered by weak allergens using the laser speckle imaging contrast technique. *Quantum Electron.* **2014**, *44*, 713–718. [CrossRef]

18. Kalchenko, V.; Kuznetsov, Y.; Preise, D.; Meglinski, I.V.; Harmelin, A. Ear swelling test by using laser speckle imaging with a long exposure time. *J. Biomed. Opt.* **2014**, *19*, 060502. [CrossRef] [PubMed]

19. Briers, J.D.; Webster, S. Laser speckle contrast analysis (LASCA): A nonscanning, full-field technique for monitoring capillary blood flow. *J. Biomed. Opt.* **1966**, *1*, 174–180. [CrossRef]

20. Sdobnov, A.; Bykov, A.; Molodij, G.; Kalchenko, V.; Jarvinen, T.; Popov, A.; Kordas, K.; Meglinski, I. Speckle dynamics under ergodicity breaking. *J. Phys. D Appl. Phys.* **2018**, *51*, 155401. [CrossRef]

21. Sdobnov, A.; Bykov, A.; Popov, A.; Zherebtsov, E.; Meglinski, I. Investigation of speckle pattern dynamics by laser speckle contrast imaging. *Proc. SPIE* **2018**, *10685*, 1068509.

22. Zakharov, P. Ergodic and non-ergodic regimes in temporal laser speckle imaging. *Opt. Lett.* **2017**, *42*, 2299. [CrossRef] [PubMed]

23. Yuan, S.; Devor, A.; Boas, D.A.; Dunn, A.K. Determination of optimal exposure time for imaging of blood flow changes with laser speckle contrast imaging. *Appl. Opt.* **2005**, *44*, 1823–1830. [CrossRef]

24. Borniger, J.C.; Teplitsky, S.; Gnyawali, S.; Nelson, R.J.; Rink, C. Photoperiodic Regulation of Cerebral Blood Flow in White-Footed Mice (Peromyscus leucopus). *eNeuro* **2016**, *3*, e0058. [CrossRef] [PubMed]

25. Hecht, N.; Woitzik, J.; Dreier, J.P.; Vajkoczy, P. Intraoperative monitoring of cerebral blood flow by laser speckle contrast analysis. *Neurosurg. Focus* **2009**, *27*, E11. [CrossRef]

26. Richards, L.M.; Towle, E.L.; Fox, D.J.; Dunn, A.K. Intraoperative laser speckle contrast imaging with retrospective motion correction for quantitative assessment of cerebral blood flow. *Neurophotonics* **2014**, *1*, 015006. [CrossRef] [PubMed]

27. Parthasarathy, A.B.; Weber, E.L.; Richards, L.M.; Fox, D.J.; Dunn, A.K. Laser speckle contrast imaging of cerebral blood flow in humans during neurosurgery: A pilot clinical study. *J. Biomed. Opt.* **2010**, *15*, 066030. [CrossRef] [PubMed]

28. Feng, N.; Qiu, J.; Li, P.; Sun, X.; Yin, C.; Luo, W.; Chen, S.; Luo, Q. Simultaneous automatic arteries-veins separation and cerebral blood flow imaging with single-wavelength laser speckle imaging. *Opt. Express* **2011**, *19*, 15777–15791. [CrossRef]

29. Postnov, D.D.; Erdener, S.E.; Kilic, K.; Boas, D.A. Cardiac pulsatility mapping and vessel type identification using laser speckle contrast imaging. *Biomed. Opt. Express* **2018**, *9*, 6388–6397. [CrossRef]

30. Ramirez-San-Juan, J.C.; Regan, C.; Coyotl-Ocelotl, B.; Choi, B. Spatial versus temporal laser speckle contrast analyses in the presence of static optical scatterers. *J. Biomed. Opt.* **2014**, *19*, 106009. [CrossRef]

31. Kirkpatrick, S.J.; Duncan, D.D.; Wells-Gray, E.M. Detrimental effects of speckle-pixel size matching in laser speckle contrast imaging. *Opt. Lett.* **2008**, *33*, 2886–2888. [CrossRef] [PubMed]

32. Schindelin, J.; Arganda-Carreras, I.; Frise, E.; Kaynig, V.; Longair, M.; Pietzsch, T.; Preibisch, S.; Rueden, C.; Saalfeld, S.; Schmid, B.; et al. Fiji: An open source platform for biological-image analysis. *Nat. Methods.* **2012**, *9*, 676–682. [CrossRef] [PubMed]

33. Davoodzadeh, N.; Cano-Velázquez, M.S.; Halaney, D.L.; Jonak, C.R.; Binder, D.K.; Aguilar, G. Evaluation of a transparent cranial implant as a permanent window for cerebral blood flow imaging. *Biomed. Opt. Express* **2018**, *9*, 4879–4892. [CrossRef] [PubMed]

34. Benmergui, A.; Drotleff, J.; Pan, T.; Zwiebel, J.; Kuznetsov, I.; Meglinski, I.; Harmelin, A.; Kalchenko, V. Machine learning assisted blood vessel segmentation in laser speckle imaging. *Proc. SPIE* **2018**, *10873*, 108730S.

35. Sdobnov, A.Y.; Darvin, M.E.; Genina, E.A.; Bashkatov, A.N.; Lademann, J.; Tuchin, V.V. Recent progress in tissue optical clearing for spectroscopic application. *Spectrochim. Acta A Mol. Biomol. Spectrosc.* **2018**, *197*, 216–229. [CrossRef]

36. Sdobnov, A.Y.; Lademann, J.; Darvin, M.E.; Tuchin, V.V. Methods for optical skin clearing in molecular optical imaging in dermatology. *Biochemistry* **2019**, *84*, 144–158. [CrossRef]

37. Kalchenko, V.; Israeli, D.; Kuznetsov, Y.; Meglinski, I.; Harmelin, A. A simple approach for non-invasive transcranial optical vascular imaging (nTOVI). *J. Biophoton.* **2015**, *8*, 897–901. [CrossRef]
38. Kalchenko, V.; Meglinski, I.; Sdobnov, A.; Kuznetsov, Y.; Harmelin, A. Combined laser speckle imaging and fluorescent intravital microscopy for monitoring acute vascular permeability reaction. *J. Biomed. Opt.* **2019**, *24*, 060501. [CrossRef]